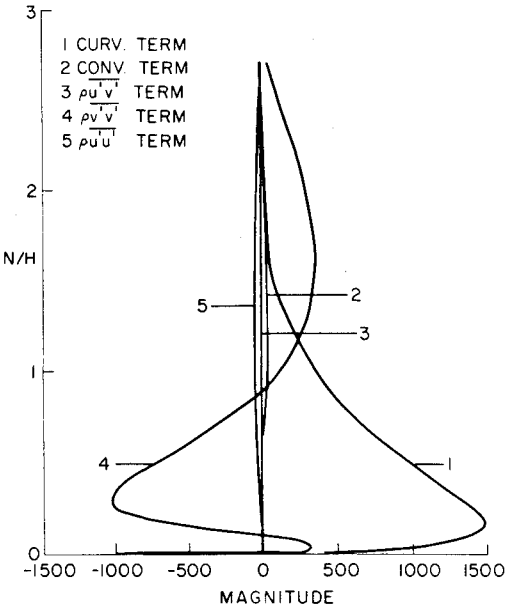

Fig. 3 Contribution of curvature, convective, and turbulent stress terms to normal pressure variation across wall jet at $S/H = 15$.

viscous/turbulence terms tend to reduce the deviation of the wall pressure from the external stream value. Note that the inviscid pressure is minimum at the peak curvature position of $S/H = 25$ while the viscous value is minimum somewhat upstream. The contribution of the various terms in the normal momentum equation to the pressure variation across the curved wall jet is exhibited in Fig. 3 at the position $S/H = 15$. The dominant term, as expected, is the surface curvature term ($K\rho U^2$). Using standard Boussinesq modeling for the turbulent stress terms, viz.

$$-\rho\overline{u_i'u_j'} = -\frac{2}{3}\rho k\delta_{ij} + \mu_t\left[\left(\frac{\partial U_i}{\partial X_j} + \frac{\partial U_j}{\partial X_i}\right) - \frac{2}{3}\operatorname{div}\bar{V}\right] \qquad (7)$$

(see Ref. 5 for the specific parabolized terms retained in curvilinear s, n coordinates) the dominant viscous contribution comes from the $\rho\overline{v'v'}$ stress term. This term acts counter to the surface curvature term over a significant portion of the wall jet. Comparable profiles at other stations and further details of this calculation are available in Ref. 9.

Concluding Remarks

The noniterative cross-flow procedure described has proven to be an efficient and reliable improvement to the two-dimensional iterative cross-flow procedure of Bradshaw and coworkers.[3,4] Comparable results with the Bradshaw method typically required two to three iterative sweeps at each station. Parabolic mixing-layer codes can be extended readily to incorporate this cross-flow procedure, and their "direct coupling" with an external potential flow solution[3,4] provides a simple extension of boundary-layer interactive concepts to situations with large normal pressure variations. The authors have formulated a "semi-iterative" extension of this approach to three-dimensional mixing-layer problems via analogous manipulations of the continuity and cross-flow momentum equations which will be described in a future article.[10]

Acknowledgments

This work was partially supported by David Taylor Naval Ship Research and Development Center under Contract N00167-83-C-0082 and by NASA Langley Research Center under Contract NAS1-16535.

References

[1] Patankar, S. V. and Spalding, D. B., "A Calculation Procedure for Heat, Mass, and Momentum Transfer in Three-Dimensional Parabolic Flows," *International Journal of Heat and Mass Transfer*, Vol. 15, Oct. 1972, pp. 1787-1806.

[2] Briley, W. R., "Numerical Method for Predicting Three-Dimensional Steady Viscous Flow in Ducts," *Journal of Computational Physics*, Vol. 14, 1974, pp. 8-28.

[3] Mahgoub, H.E.H. and Bradshaw, P., "Calculation of Turbulent-Inviscid Flow Interactions with Large Normal Pressure Gradients," *AIAA Journal*, Vol. 17, Oct. 1979, pp. 1025-1029.

[4] Chen, Z. B. and Bradshaw, P., "Calculation of Viscous Transonic Flow Over Airfoils," *AIAA Journal*, Vol. 22, Feb. 1984, pp. 201-205.

[5] Dash, S. M., Beddini, R. A., Wolf, D. E., and Sinha, N., "Viscous/Inviscid Analysis of Curved Sub- or Supersonic Wall Jets," *AIAA Journal*, Vol. 23, Jan. 1985, pp. 12-13; also, AIAA Paper 83-1679, July 1983.

[6] Dash, S. M. and Wolf, D. E., "Interactive Phenomena in Supersonic Jet Mixing Problems, Part I: Phenomenology and Numerical Modeling Techniques," *AIAA Journal*, Vol. 22, July 1984, pp. 905-913.

[7] Dash, S. M. and Wolf, D. E., "Fully-Coupled Analysis of Jet Mixing Problems, Part I: Shock-Capturing Model, SCIPVIS," NASA CR 3761, Jan. 1984.

[8] Launder, B. E., Priddin, C. H., and Sharma, B. I., "The Calculation of Turbulent Boundary Layers on Spinning and Curved Surfaces," *ASME Journal of Fluids Engineering*, Vol. 99, March 1977, pp. 231-239.

[9] Dash, S. M. and Sinha, N., "Pressure-Split Extensions of SPLITWJET Model for Wall Jet/Potential Flow Coupling," Science Applications, Inc., Princeton, N.J., SAI/PR TR-17, Feb. 1984.

[10] Dash, S. M., Wolf, D. E., and Sinha, N., "Parabolized Navier-Stokes Analysis of Three-Dimensional Jet Mixing Problems," AIAA Paper 84-1525, June 1984.

Emmons Spot Forcing for Turbulent Drag Reduction

Wesley L. Goodman*
NASA Langley Research Center, Hampton, Virginia

Nomenclature

$C_F/C_{F_{HF}}$	= skin-friction coefficient normalized by skin-friction coefficient at maximum frequency
f	= frequency, Hz
R_θ	= Reynolds number based on momentum thickness
St	= Strouhal number, $= f\delta/U\infty$
U_∞	= freestream velocity
V_w'	= acoustic perturbation velocity
Z	= transverse coordinate
δ	= boundary-layer thickness
θ	= boundary-layer momentum thickness

Introduction

THE viscous or skin-friction drag associated with a turbulent boundary layer accounts for approximately 50% of the drag on conventional takeoff and landing (CTOL) aircraft and surface ships and nearly all of the pumping power in long-distance pipelines. Reduction of this viscous drag would allow longer range, reduced fuel volume/cost, and/or

Received Oct. 4, 1983. Revision received Jan. 23, 1984. This paper is declared a work of the U.S. Government and therefore in the public domain.

*Aerospace Engineer, Turbulent Drag Reduction Group, Viscous Flow Branch, High-Speed Aerodynamics Division.

increased speed. As an example, a 20% reduction in fuselage skin-friction drag on U.S. CTOL civilian aircraft translates into a yearly fuel savings approaching $1 billion, an estimate that does not include the additional savings and increased performance from either the Department of Defense or surface ship and pipeline applications.[1]

A promising viscous drag reduction technique is the modification of the large-scale eddy structure in the turbulent boundary layer. Reference 2 has found that large-scale eddy modification can lead to reduced skin friction and that the modified structure has a very long "healing" distance downstream. Reference 3 indicates that, for at least $R_\theta < 5 \times 10^3$, the large eddy structure of the turbulent boundary layer is produced by the Emmons spot generation process (e.g., during transition). The purpose of the present investigation was to attempt to produce local skin-friction reduction through alteration of these Emmons spot-induced structures. Reference 4 has shown that the growth of these Emmons spots can be modified by altering the spot-to-spot proximity. Therefore, the present investigation attempted to produce small turbulence scales in the initial region of the turbulent boundary layer via closely spaced Emmons spot triggers operating at high frequency. Previous attempts at altering the Emmons spot structure include Ref. 5. However, this work did not incorporate the concepts of closely spaced, high-frequency triggering [$\Delta z/\delta \sim \mathcal{O}(1), f\delta/U_\infty \sim \mathcal{O}(1)$].

Emmons Spot Generating System

A preliminary study was conducted in the Langley 7 × 11 in. low-speed wind tunnel at a freestream velocity of 7.62 m/s. An Emmons spot-generation system was designed to produce very closely spaced [$\Delta z/\delta \sim \mathcal{O}(1)$] Emmons spots in the spanwise direction. For high Strouhal numbers (St), these initial experiments yielded shape factors indicating a much more rapid transition process. Also, the momentum thickness distributions indicated local skin-friction reductions and a possible "net" skin-friction reduction at the end of the test section. Although the results showed some promise for the approach (Emmons spot forcing), there were inherent problems in these initial experiments. For example, an auxiliary two-dimensional trip rod was installed upstream of the test section to "fix" the nominal location of the transition at the location of the Emmons spot triggers. It is possible that the induced dynamic (acoustic) disturbance due to the trigger system coupled with the two-dimensional trip disturbance field to give a transition process peculiar to this particular "combined trip."

A more detailed investigation was therefore conducted in the Langley 15 in. low-turbulence wind tunnel at a freestream velocity of 3.05 m/s [note, $U'_\infty/U_\infty \sim \mathcal{O}(0.03\%)$]. As shown in Fig. 1, the Emmons spot triggers were located 157.48 cm downstream of the beginning of the test section. Note that there is a boundary-layer suction slot at the beginning of the test section in order to eliminate the boundary layer developed in the wind tunnel contraction. The Emmons spot trigger apparatus consisted of a single spanwise row of holes with two acoustic horn drivers (connected in parallel and matched in amplitude) mounted underneath. Hole size and spacing were varied parametrically. Both 30 and 75 W horn drivers were employed. A spanwise uniform perturbation velocity field was obtained by varying the cavity geometry under the surface holes and the spacing of the horn drivers. The data consisted of both pilot-profile surveys of the boundary layer and direct-drag measurements. The drag measurements were made on a 91.44 cm plate that spanned the test section (see Ref. 6 for details of the drag balance.)

This experiment was quite difficult to conduct due to the necessity of having an acoustic perturbation velocity V'_w on the order of 20% of the freestream velocity [i.e., $V'_w/U_\infty \sim \mathcal{O}(0.20)$] in order to generate the Emmons spots (see Ref. 7) coupled with the basic experimental requirement of high-frequency [$f\delta/U_\infty \sim \mathcal{O}(1)$] triggering. Based on initial smoke tests, these ground rules led to a freestream velocity of 3.05 m/s.

With such a low freestream velocity the drag levels, even when averaged over the large drag plate area, are quite low, with consequent accuracy difficulties. In an attempt to determine and quantify data consistency, multiple runs were made at a given condition and the drag results were normalized to the results at maximum frequency. This was based upon the following physical picture. At zero frequency, the flow over the drag balance plate was partially laminar. When the drivers were actuated, smoke data indicated that a certain amplitude was required to trip the flow at the driver location ($V'_w/U_\infty \simeq 0.195$). At this amplitude and a midrange of frequencies [corresponding to Strouhal number $\mathcal{O}(1)$], both quantitative and qualitative results indicate smaller turbulence scales and a reduction in skin-friction drag. For low frequencies, there was greater spacing between the spots in the streamwise direction and therefore they were not as constrained in size, which allowed larger-scale motions. For high frequencies, the driver influence should be confined to the very near wall region and therefore the drivers should act merely as a massive tripping device, rather than as individual Emmons spot generators. Local skin-friction reductions $\mathcal{O}(15\%)$ were observed in the present studies (see Fig. 2, where the shaded area indicates the data spread for repeat runs). The data shown in Fig. 2 were corrected to the same R_θ using an empirical variation of C_f with R_θ ($C_f \sim R_\theta^{0.272}$).[8] The level of C_f reduction noted on Fig. 2 (15%) is the same order as usually obtained with large-eddy breakup devices (see Fig. 24 in Ref. 9).

Measurements of the momentum thickness (θ) of the boundary layer over the drag balance flat plate were made at the front and rear of the plate. The trends of the curves of θ vs frequency were the same for both ends of the plate for a given test condition. The variation of θ with frequency at the front of the plate is shown in Fig. 3. These measurements of θ,

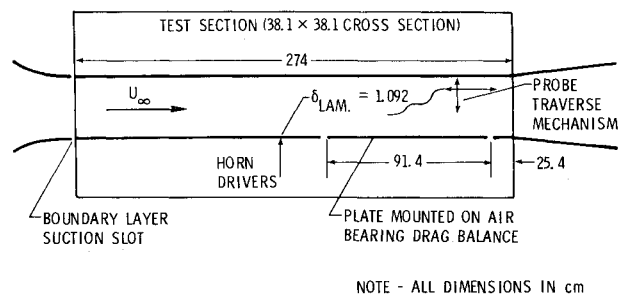

Fig. 1 Schematic of experimental setup.

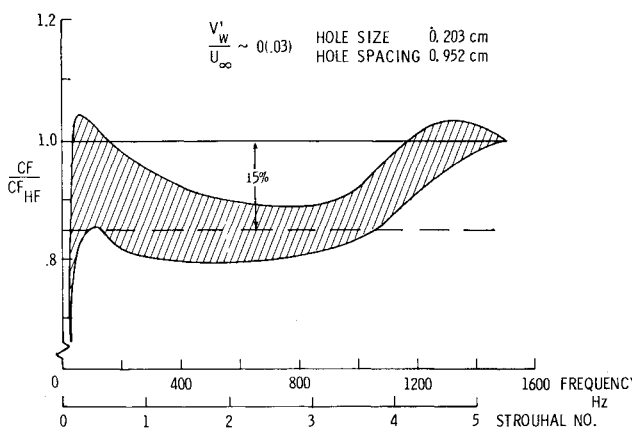

Fig. 2 Normalized skin friction as a function of frequency.

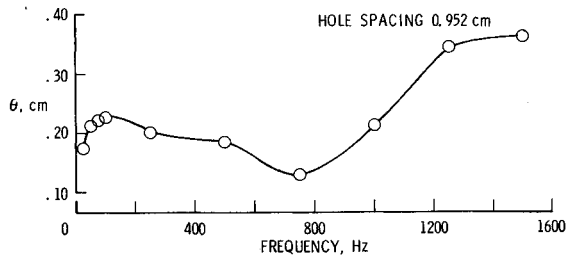

Fig. 3 Momentum thickness as a function of frequency.

along with the vertical and horizontal smoke wire pictures, indicate that the area-averaged drag reductions are not just a result of a shift in the transition region location (e.g., thicker boundary layer), but are most probably a result of the production of smaller turbulence scales.

As stated earlier, the purpose of this investigation was to attempt to produce local skin-friction reduction through alteration of the Emmons spot structures. Having produced such a drag reduction, it is of interest to examine the overall efficiency of such an approach. The expected longitudinal extent of the skin-friction reduction is of $\mathcal{O}(120\delta)$.[10] Based on this length, the power saved is of $\mathcal{O}(5.27\times10^{-3}$ W). The power required to run the acoustic horn driver trigger is of $\mathcal{O}$(3.16 W). Obviously, the present trigger system does not allow a net reduction; however, other, perhaps passive, trigger approaches may do so.

Conclusions

In summary, an Emmons spot generation system was designed to trigger closely spaced Emmons spots in the spanwise and longitudinal directions. For certain combinations of generator frequencies and amplitude, hole size, and hole spacing, quantitative and qualitative results indicate smaller turbulence scales and a reduction in skin friction [of $\mathcal{O}$(15%)]. This reduction in local drag does not appear to be a result of simply shifting the transition region location. The efficiency of the present trigger system does not allow a net drag reduction. However, other, perhaps passive, trigger approaches may do so.

References

[1] Bushnel, D.M., "Turbulent Drag Reduction for External Flows," AIAA Paper 83-0227, Jan. 1983.

[2] Corke, T.C., Nagib, H.M., and Guezennec, Y.G., "A New View on Origin, Role and Manipulation of Large Scales in Turbulent Boundary Layers," Illinois Institute of Technology, Chicago, NASA CR 165861, Feb. 1982.

[3] Zilberman, M., Wygananski, I., and Kaplan, R.E., "Transitional Boundary Layer Spot in a Fully Turbulent Environment," Paper presented at IUTAM Symposium 1976, Structure of Turbulence and Drag Reduction; also *Physics of Fluids*, Vol. 20, Oct. 1977, pp. S258-S276.

[4] Savas, O., "Some Measurements in Synthetic Turbulent Boundary Layers," *Turbulent Boundary Layer: Experiments, Theory, and Modeling*, AGARD CP 271, Jan. 1980, Paper 23, pp. 23-1-23-12.

[5] Chamber, F.W., "Preliminary Measurements of a Synthetic Turbulent Boundary Layer," Lockheed-Georgia Paper LG82RR0009, Sept. 1982.

[6] Lin, J.C, Walsh, M.J., Watson, R.D. and Balasubramanian, R., "Turbulent Drag Characteristics of Small Amplitude Rigid Surface Waves," AIAA Paper 83-0228, Jan. 1983.

[7] Elder, J.W., "An Experimental Investigation of Turbulent Spots and Breakdown to Turbulence," *Journal of Fluid Mechanics*, Vol. 9, 1960, pp. 235-246.

[8] Klabanoff, P.S., "Characteristics of Turbulence in a Boundary Layer with Zero Pressure Gradient," NACA TN 3178, 1954.

[9] Hefner, J.N., Anders, J.B. and Bushnell, D.M., "Alteration of Outer Flow Structures for Turbulent Drag Reduction," AIAA Paper 83-0293, Jan. 1983.

[10] Anders, J.B., private communication, Aug. 1983.

Boundary-Layer Blowing

Ravi Bahl*
Technical Teachers' Training Institute
Chandigarh, India

Introduction

HAVING worked on external flow problems[1,2] the author has applied the method developed previously to investigate two-dimensional boundary-layer separation and attachment due to small blowing through a transverse porous slot. Steady-state Navier-Stokes equations are taken as the governing equations for the fluid motion, and appropriate boundary conditions are used. The flow is assumed to be incompressible and laminar to simplify the problem.

The geometrical representation of the flow problem is shown in Fig. 1. Flat plate 4 is assumed to be placed parallel to the flow stream. The flow takes place from left to right. At point 5 there is a porous slot through which small blowing occurs. The flow on the upstream side (1) of the flat plate is a similarity solution of Blasius[3] and it is assumed that blowing does not influence the upstream boundary condition. At the top of the plate, i.e., boundary 2, the normal derivative of stream function ψ gives freestream velocity U, and the normal derivative of vorticity is taken as zero. On the downstream boundary 3, the values of vorticity and stream function are extrapolated according to Adam's predictor-corrector scheme.[4] On the surface of the flat plate, i.e., boundary 4, no-slip conditions exist and the normal component of velocity is zero. At the porous slot, i.e., boundary 5, uniform upward velocity exists and the component of velocity along the plate is zero.

Governing Equations

The Navier-Stokes equations governing the steady, incompressible viscous motion of fluid without body force can be written as

$$\nabla^2\psi+\zeta=0 \tag{1}$$

$$\nabla^2\zeta+Re\left(\frac{\partial\psi}{\partial y}\frac{\partial\zeta}{\partial x}-\frac{\partial\psi}{\partial x}\frac{\partial\zeta}{\partial y}\right)=0 \tag{2}$$

Equation (1) is known as the stream function equation and Eq. (2) as the vorticity equation. The coordinates x and y are stretched using a simple transformation and the resulting equations are written in finite difference form. The finite difference equations are solved by a modified version of the extrapolated Liebmann method.[1,2]

Results and Discussion

Before attempting to solve the problem of boundary-layer blowing, a simple problem of laminar steady flow over a flat plate is examined at a plate Reynolds number of order 10^4. The reason for solving flow over a flat plate is to establish the validity of technique and compare the results with well-known and established results; as follows.

The no-slip and zero normal velocity boundary condition is applied along the entire flat plate for this case with the other boundary conditions described previously. After some numerical experimentation a grid of 64×32 was chosen. The results obtained compared to within 3% with Blasius

Received Nov. 29, 1983; revision received Feb. 22, 1984.

*Assistant Professor, Mechanical Engineering Department.